

1990

$H_{\text{at}}$  represents the usual non-relativistic free atom Hamiltonian, in which the electrostatic particle mass renormalization has been taken into account.  ${}^{(L)}H^{(r)}$  is the “instantaneous” electrostatic atom–cavity wall coupling term (whose exact form depends upon the cavity geometry). This term appears here as an atomic operator.  ${}^{(T)}H$  represents the free transverse field Hamiltonian given by eq. (2.10).  $H_I + H_{II}$  describes the coupling between the atom and the transverse field in the cavity. It also depends upon the cavity geometry, since  $A$  is a sum over the cavity modes. This coupling is the sum of a term  $H_I$  linear in  $a_\mu$  and  $a_\mu^\dagger$  and of a term  $H_{II}$  quadratic in  $a_\mu, a_\mu^\dagger$ . For sake of simplicity, we will in the following restrict the discussion to a one electron atom and perform the electric dipole approximation justified by the fact that the atom size is very small compared to the field wavelengths. We can then replace in  $H_I + H_{II}$  the  $\mathbf{r}_\alpha$ 's by the position  $\mathbf{R}$  of the atom center of mass and we finally get

$$H = (m + \delta m)c^2 + \frac{p^2}{2m} + V_{\text{coul}}(\mathbf{r}) + \sum_{\mu} \hbar\omega_{\mu} \left( a_{\mu}^{\dagger} a_{\mu} + \frac{1}{2} \right) + {}^{(L)}H^{(r)}(\mathbf{R}) - \frac{q}{m} \mathbf{p} \cdot \mathbf{A}(\mathbf{R}) + \frac{q^2}{2m} A^2(\mathbf{R}). \quad (2.19)$$

### 2.3. Counting modes between two mirrors: the Casimir effect

As a simple introduction to cavity QED effects we first describe the transverse field modes in a “prototype” cavity made of two plane parallel mirrors and we consider a situation where there is no atom inside. The Casimir effect, namely the occurrence of a vacuum radiation pressure between the mirrors, results from the change in the mode distribution brought about by the boundaries. We present a simple derivation of this effect and discuss on this elementary example some of the basic ideas of the cavity QED renormalization procedure.

The “mirror gap cavity” is shown in fig. 10. The mirrors are in the  $z = 0$  and  $z = L$  planes and the cavity “volume” is the  $0 < z < L$  infinite slab. The cavity modes are divided into transverse electric (TE) and transverse magnetic (TM) modes having their electric field and magnetic field, respectively, parallel to the surface. These modes are superpositions of plane waves bouncing on the surfaces with wave vectors  $\mathbf{k}_+$  and  $\mathbf{k}_-$  having equal components along the mirrors and opposite components along the  $z$  axis:

$$\mathbf{k}_{\pm} = \mp l \mathbf{n} + k \boldsymbol{\varphi}. \quad (2.20)$$

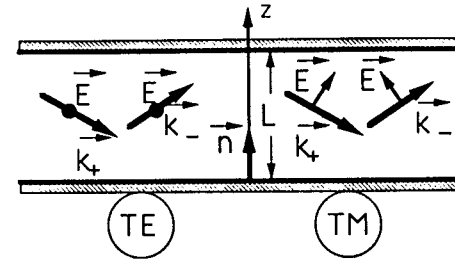


Fig. 10. Cross section of cavity made of two parallel mirrors with representation of the wave vectors and electric fields in the TE and TM mode configurations.

$\mathbf{n}$  is the unit vector normal to the mirrors and  $\boldsymbol{\varphi}$  the unit vector parallel to the mirror along the direction defined by the azimuthal angle  $\varphi$ .  $l, k$  and  $\varphi$  are the cylindrical coordinates of the  $\mathbf{k}$  wave vectors and  $l$  and  $k$  are related to the mode frequency  $\omega$  by the relation

$$\frac{\omega^2}{c^2} = l^2 + k^2. \quad (2.21)$$

The total electric field component along the mirrors and the magnetic field component normal to the surfaces vanish at  $z = 0$  and  $z = L$ . These boundary conditions impose the quantization of  $l$ :

$$l = m\pi/L, \quad (2.22)$$

so that eq. (2.21) becomes

$$\omega^2 = m^2 \omega_0^2 + k^2 c^2, \quad (2.23)$$

with

$$\omega_0 = c\pi/L. \quad (2.24)$$

The normalized field distributions for the TE and TM modes correspond to linear superpositions of plane waves with  $\mathbf{k}_+$  and  $\mathbf{k}_-$  wave vectors. We obtain:

$$\alpha_{m,k,\varphi}^E(z, \boldsymbol{\varrho}) = \left( \frac{2}{V} \right)^{1/2} \sin \frac{m\pi z}{L} e^{ik\boldsymbol{\varphi} \cdot \boldsymbol{\varrho}} \boldsymbol{\varphi} \times \mathbf{n}, \quad (2.25a)$$

$$\alpha_{m,k,\varphi}^M(z, \boldsymbol{\varrho}) = \left( \frac{\beta_m}{V} \right)^{1/2} \left[ \frac{ck}{\omega} \cos \frac{m\pi z}{L} \mathbf{n} - i \frac{m\omega_0}{\omega} \sin \frac{m\pi z}{L} \boldsymbol{\varphi} \right] e^{ik\boldsymbol{\varphi} \cdot \boldsymbol{\varrho}} \quad (2.25b)$$

with

$$\beta_m = 1 \text{ if } m = 0; \quad \beta_m = 2 \text{ if } m > 0. \quad (2.25c)$$

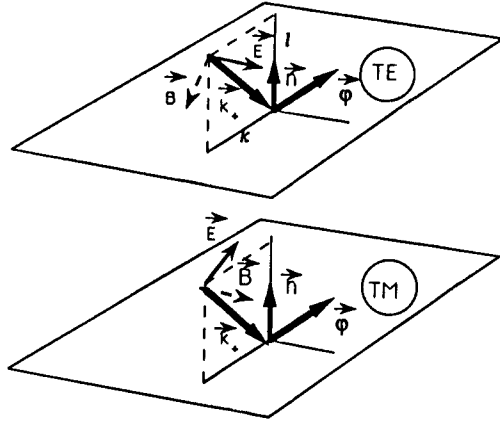


Fig. 11. Three-dimensional representation of the  $k$ ,  $E$  and  $B$  vectors for the TE and TM modes in front of a plane mirror.

We have adopted for  $\mathbf{r}$  the cylindrical coordinate notation ( $\varrho$  is the projection of  $\mathbf{r}$  along the mirrors). The disposition of  $\mathbf{n}$ ,  $\varphi$ ,  $E$  and  $B$  vectors in each of these modes is shown in fig. 11 for TE and TM modes.  $V$  is an arbitrary "quantization" volume introduced here for mode normalization. This volume is for example a rectangular box of height  $L$  in the  $z$  direction, with sides of arbitrary length  $a$  in the  $x$  and  $y$  directions ( $V = La^2$ ). Note that the normalization is different for  $m = 0$  and  $m > 0$  modes.  $m = 0$  modes have no spatial variation along  $z$  and, since the transverse component of the electric field vanishes for  $z = 0$  and  $z = L$ , they must have zero transverse electric field everywhere in the gap. There is thus no TE mode with  $m = 0$ . According to eq. (2.23) the smallest possible TE mode frequency is  $\omega_0$ , which is called the TE cutoff frequency of the gap. The TM modes with  $m = 0$  have a uniform field distribution and a normalization factor equal to  $(1/V)^{1/2}$  whereas all the other modes (for which the square of the sine and cosine function average to 1/2 in the cavity) have a normalization factor  $(2/V)^{1/2}$ . Plugging the mode functions in eq. (2.5), we separate the vector potential operator as a sum of TE and TM contributions:

$$A(z, \varrho) = A^E(z, \varrho) + A^M(z, \varrho), \quad (2.26)$$

with

$$A^E(z, \varrho) = \sum_{m,k,\varphi} \left\{ \sqrt{\frac{\hbar}{2\varepsilon_0\omega}} \alpha_{m,k,\varphi}^E(z, \varrho) a_{m,k,\varphi}^E + \text{h.c.} \right\}, \quad (2.27)$$

$$A^M(z, \varrho) = \sum_{m,k,\varphi} \left\{ \sqrt{\frac{\hbar}{2\varepsilon_0\omega}} \alpha_{m,k,\varphi}^M(z, \varrho) a_{m,k,\varphi}^M + \text{h.c.} \right\}. \quad (2.28)$$

$a_{m,k,\varphi}^E$  and  $a_{m,k,\varphi}^M$  are the photon annihilation operators in the TE and TM modes. The frequency  $\omega$  in eqs. (2.27, 28) is of course related to  $m$  and  $k$  by eq. (2.23).

In order to count the modes, we adopt cyclic boundary conditions for the transverse wave vector components  $k_x$  and  $k_y$ , which are quantized in units of  $2\pi/a$ . The unit cell in the transverse reciprocal plane has then an area  $(2\pi)^2/a^2$  and the number of TE or TM modes with a given  $m$  and their transverse wave vector coordinates in the interval  $k, k + dk$  is  $a^2 k dk/2\pi$ .

Differentiating eq. (2.23) we remark that  $k dk = (1/c^2)\omega d\omega$  and thus the number of TE or TM modes with a given  $m$  and a frequency  $\omega$  between  $\omega$  and  $\omega + d\omega$  is  $(a^2/c^2)\omega d\omega/2\pi$ . According to eq. (2.23), a given  $\omega$  value can be obtained with  $m$  varying from 0 up to  $\text{Int}(\omega/\omega_0)$ , where  $\text{Int}()$  denotes the integer part function. Finally, for each set of  $m, k, \varphi$  values with  $m > 0$ , there is one TE and one TM mode and only one TM mode if  $m = 0$ . Thus the number of modes in a unit frequency interval at frequency  $\omega$ , which we call the mode spectral density  $\rho^{(\text{cav})}(\omega)$  is

$$\rho^{(\text{cav})}(\omega) = \frac{a^2\omega}{2\pi c^2} \left[ 1 + 2 \text{Int} \left( \frac{\omega}{\omega_0} \right) \right]. \quad (2.29)$$

This expression can be written in a slightly different way by introducing the cavity volume  $V = La^2$  and by replacing  $\text{Int}(\omega/\omega_0)$  by a sum of Heaviside functions  $\Theta(\omega/\omega_0 - m)$  ( $\Theta$  is equal to one if its argument is strictly positive, to zero otherwise):

$$\rho^{(\text{cav})}(\omega) = \frac{V\omega\omega_0}{2\pi^2 c^3} \left[ 1 + 2 \sum_{m=1}^{\infty} \Theta \left( \frac{\omega}{\omega_0} - m \right) \right]. \quad (2.30)$$

The free-space density is recovered by letting  $L$  go to infinity. Then  $\omega_0 \rightarrow 0$  and  $\rho^{(\text{cav})}(\omega)$  reduces to the well known expression

$$\rho^{(0)}(\omega) = \frac{V\omega^2}{\pi^2 c^3}. \quad (2.31)$$

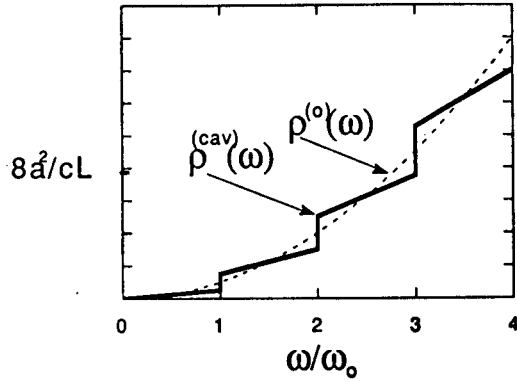


Fig. 12. The mode spectral density  $\rho^{(cav)}(\omega)$  as a function of angular frequency  $\omega$  in the plane parallel mirror gap (solid line).  $\omega$  is measured in units of the gap cutoff frequency  $\omega_0$ . The modes are counted in a box of volume  $a^2L$ . The free-space mode density is represented as a dashed line for comparison.

Figure 12 displays the mode spectral density in the gap (solid line) and in free-space (dashed line) as a function of  $\omega$ . The two densities are very different from each other for  $\omega$  smaller than or of the order of  $\omega_0$ . The relative difference between the two densities becomes small at frequencies large compared to  $\omega_0$ . We thus expect that physical effects related to the cavity induced change in the mode density essentially come from the contribution of frequencies up to a few  $\omega_0$ .

We now proceed to compute the Casimir effect [2,66,67]. The change of the mode spectral distribution with  $L$  entails a variation of the total field vacuum energy versus the gap separation and hence results in the existence of a force pulling the mirrors together. The vacuum field energy  $W(L)$  in a section  $a^2$  of the gap is

$$W(L) = \int_0^{+\infty} \frac{\hbar\omega}{2} \rho^{(cav)}(\omega) d\omega = \frac{a^2\hbar}{4\pi c^2} \left[ I_0 + 2 \sum_{m=1}^{\infty} I_m \right], \quad (2.32)$$

with  $I_m$  defined as

$$I_m = \int_{m\omega_0}^{+\infty} \omega^2 d\omega. \quad (2.33)$$

$W(L)$  obviously diverges, due to the contribution of the high frequency modes. The divergence of  $I_0$  is not a problem since only the part of  $W(L)$  which depends upon  $L$  is physically significant. As for the  $I_m$  ( $m \neq 0$ )

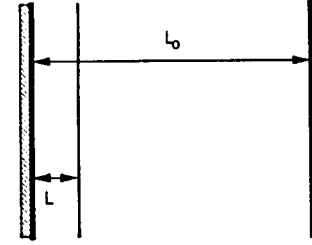


Fig. 13. Sketch of the mirror configuration considered in the derivation of the Casimir interaction between plates: the gap of width  $L$  is embedded in a larger gap of width  $L_0$ . The variation of the field energy with the position of the intermediate mirror is the relevant physical quantity.

integrals, we will compute them by multiplying the integrand by a converging term  $e^{-\lambda\omega/c}$  whose physical meaning will be discussed later. We will check at the end of the calculations that the final result has a well-defined limit for  $\lambda \rightarrow 0$ . We get the following expression for  $I_m$ ,

$$\begin{aligned} I_m &= \int_{m\pi c/L}^{+\infty} \omega^2 e^{-\lambda\omega/c} d\omega \\ &= c^2 \frac{\partial^2}{\partial \lambda^2} \int_{m\pi c/L}^{+\infty} e^{-\lambda\omega/c} d\omega \\ &= c^3 \frac{\partial^2}{\partial \lambda^2} \left[ -\frac{e^{-m\pi\lambda/L}}{\lambda} \right], \end{aligned} \quad (2.34)$$

and for the sum over  $m$ ,

$$\begin{aligned} \sum_{m=1}^{\infty} I_m &= -c^3 \frac{\partial^2}{\partial \lambda^2} \left\{ \sum_{m=1}^{\infty} \frac{e^{-m\pi\lambda/L}}{\lambda} \right\} \\ &= \frac{c^3\pi}{L} \frac{\partial^2}{\partial \lambda^2} \left\{ \frac{1}{\pi\lambda/L} \frac{1}{e^{\pi\lambda/L} - 1} \right\}. \end{aligned} \quad (2.35)$$

The asymptotic expansion of the bracketed function in eq. (2.35) writes

$$\frac{1}{\pi\lambda/L} \frac{1}{e^{\pi\lambda/L} - 1} = \frac{1}{(\pi\lambda/L)^2} - \frac{1}{2\pi\lambda/L} + \frac{1}{12} - \frac{1}{720} \left( \frac{\pi\lambda}{L} \right)^2 + \dots \quad (2.36)$$

Combining then eqs. (2.32), (2.35) and (2.36) we get

$$W(L) = \frac{a^2\hbar}{4\pi c^2} I_0 + \frac{a^2\hbar c}{2} \left[ \frac{6L}{\pi^2\lambda^4} - \frac{1}{\pi\lambda^3} - \frac{2\pi^2}{720L^3} + \dots \right]. \quad (2.37)$$

Consider now that the gap  $L$  is embedded in a larger gap of width  $L_0 \gg L$ , with the two extreme mirrors being fixed and the intermediate movable mirror reflecting the field on both sides (see fig. 13) and let us determine the total change in vacuum energy when  $L$  is varied. Adding the contributions of the  $L$  and  $L - L_0$  gaps, we immediately get the total energy  $W_T(L)$ :

$$W_T(L) = \frac{a^2 \hbar}{2\pi c^2} I_0 + \frac{a^2 \hbar c}{2} \left[ \frac{6L_0}{\pi^2 \lambda^4} - \frac{2}{\pi \lambda^3} - \frac{2\pi^2}{720 L^3} + \dots \right]. \quad (2.38)$$

We have neglected in eq. (2.38) the contribution  $1/(L_0 - L)^3$ , which is very small compared to the  $1/L^3$  term. For a different configuration  $\{L', L_0 - L'\}$ ,  $W_T(L')$  is given by the same expression with  $L$  replaced by  $L'$  and the change in the system energy is

$$W_T(L') - W_T(L) = -\frac{a^2 \pi^2 \hbar c}{720} \left( \frac{1}{L'^3} - \frac{1}{L^3} \right). \quad (2.39)$$

The system has thus a  $\lambda$  independent potential energy  $U(L)$  given by

$$U(L) = -\frac{\pi^2 \hbar c}{720} a^2 \frac{1}{L^3}. \quad (2.40)$$

There is consequently a vacuum pressure  $P_{\text{vac}}$  pulling the plates together:

$$P_{\text{vac}} = \frac{1}{a^2} \frac{\partial U}{\partial L} = \frac{\pi^2 \hbar c}{240} \frac{1}{L^4}. \quad (2.41)$$

The order of magnitude of this vacuum pressure is very small, about  $10^{-3}$  Pa for  $L = 1$  mm. It is equivalent to the electrostatic pressure experienced by metallic plates charged with one electron per  $L^2$  area! Attractive forces between plates related to this tiny interaction have been measured [68-69].

Let us come back to the physical significance of the mathematical trick we used to get a converging result for  $P_{\text{vac}}$ . Introducing the exponential cutoff function  $e^{-\lambda\omega/c}$  amounts to suppressing the contribution to the Casimir effect of modes with wavelengths shorter than  $\lambda$ . This means that the presence of the metallic boundaries makes no difference for the mode density at short wavelengths. In fact, all real mirrors do have a plasma cutoff frequency above which they are transparent, so that it is natural to assume that the actual mode density cannot be altered above a finite frequency. In other terms, the converging factor has a physical justification. A more physical cutoff procedure, taking also into account explicitly the dephasing of the field on real mirrors has recently been performed on the Casimir

problem [70]. The fact that the result of the calculation is independent of  $\lambda$  means that the Casimir effect does not depend upon the nature of the mirrors, provided their cutoff frequency corresponds to wavelengths much shorter than  $L$ . The system we considered to compute the vacuum pressure between the plates (see fig. 13) is quite similar to an osmotic pressure device. The intermediate moving mirror acts as a piston impermeable to low frequency photons but transparent to high frequency ones. We will introduce similar converging factors in integrals appearing in the expression of cavity QED level shifts, with basically the same justification. The results will again be insensitive to the details of the cutoff, which will ultimately justify the fact that cavity QED can be to a large extent discussed without having to define the nature of the cavity walls.

#### 2.4. Radiation of atoms in a cavity: modification of spontaneous emission rates

The cavity walls around the atom modify the atomic energy levels and the spontaneous emission rates of atomic excited states. We first analyze the latter effect. Consider an excited eigenstate  $|a\rangle$  of the atomic Hamiltonian  $H_{\text{at}}$  connected to lower states  $|j\rangle$  by a non vanishing matrix element of the electron momentum operator  $\mathbf{p}$ . Spontaneous emission corresponds to the transition  $|a, \text{vacuum}\rangle \rightarrow |j; 1 \text{ photon in mode } \mu, \text{ frequency } \omega_\mu\rangle$  (fig. 14a). This process is induced by the  $H_I = -(q/m)\mathbf{A} \cdot \mathbf{p}$  term of the atom-field Hamiltonian. If the cavity provides a continuum of modes for the emitted photon (wave guide structure or "moderate  $Q$ " cavity), the emission process is irreversible and the decay rate depends upon the density  $\rho^{(\text{cav})}(\omega_{aj})$  of photon modes at frequency  $\omega_{aj}$  (number of modes per unit frequency interval at  $\omega = \omega_{aj}$ ). Describing the bandwidth  $\Gamma_\mu$  of each mode in a simple phenomenological way, we can write the mode density as

$$\rho^{(\text{cav})}(\omega) = \sum_{\mu} \delta_{\Gamma_\mu}(\omega - \omega_\mu), \quad (2.42)$$

where  $\delta_{\Gamma_\mu}$  is the normalized Lorentz function of width  $\Gamma_\mu$  introduced in section 1. The total decay rate  $\gamma_{a \rightarrow j}^{(\text{cav})}$  from level  $a$  to  $j$  is obtained by using the Fermi Golden rule:

$$\gamma_{a \rightarrow j}^{(\text{cav})} = \frac{2\pi}{\hbar^2} \sum_{\mu} |\langle a, 0 | H_I | j, 1_\mu \rangle|^2 \delta_{\Gamma_\mu}(\omega_{aj} - \omega). \quad (2.43)$$

Replacing in this equation  $H_I$  by its expression and using the expansion